NUMERICAL ANALYSIS OF INITIAL STAGE OF PLATE IMPACT ON WATER SURFACE

A. Iafrati, INSEAN (Italian Ship Model Basin), Rome, Italy,
A. A. Korobkin, Lavrentyev Institute of Hydrodynamics, Novosibirsk, Russia
E-mail: a.iafrati@insean.it, kaa@hydro.nsc.ru

SUMMARY

The hydrodynamic loads originated during the water entry of a two-dimensional flat plate are investigated. The plate is initially floating on the free surface and is assumed to start suddenly its vertical motion. The liquid is ideal and incompressible, and gravity and surface tension effects are not taken into account. A numerical model able to describe the unsteady free surface flow generated by the plate impact is developed and the resulting hydrodynamic loads are estimated. The latter are compared with their asymptotic behaviour for small time, derived in a previous work. It is shown that, aside from an initial transient during which the numerical solution is not available, the theoretical estimate of the loads very well agrees with the numerical results, at least until the plate depth is of the order of 1/100 of the plate breadth. Subsequently the theoretical estimate is no longer reliable as the assumptions made in their derivation are no longer valid.

1. INTRODUCTION

The sudden vertical motion of a two-dimensional plate initially floating on a still liquid surface is considered. It is assumed that no air is entrained at the plate-liquid interface, and that the liquid flow is plane, symmetric and potential. Both surface tension and the gravity are not taken into account. The liquid is assumed ideal and incompressible. A numerical model able to describe the fully nonlinear, unsteady free-surface flow generated by the plate motion is developed and the resulting hydrodynamic loads are estimated. The numerical results are compared with the theoretical estimates derived in [1].

The motivation for the activity stems from the difficulties that standard potential flow solvers have in accurately describing the very initial stage of the plate impact. Despite the short duration, very high hydrodynamic loads are generated in the early stage, which cannot be accurately predicted by a numerical tool. Similarly to what has been done for the floating wedge case [2], it is here proposed to use the initial asymptotic estimate derived in [1] until the numerical results become available and reliable.

On the basis of the above consideration, a numerical model able to describe the unsteady free-surface flow generated by the plate impact is here developed. The model is based on a classical mixed Eulerian-Lagrangian approach with the velocity potential assigned on the free surface and its normal derivative assigned on the plate boundary. About the plate edge, the flow is complicated by the interaction between the fluid escaping from the bottom of the plate and the vertical flow at the free surface, which gives rise to thin jets [3]. In order to properly describe this interaction, additional conditions are enforced at the plate edge requiring that the free surface is attached to the plate egde and the fluid leave the plate tangentially.

In the very initial transient the conditions at the plate edges and the formation of the thin jets make the development of a reliable numerical model very complicated. In order to overcome those problems, we decided to use the small time solution derived in [3] to provide an initial shape of the free surface shape and a distribution of the velocity potential along it. To this aim, an initial time t^* is chosen to scale the self-similar variable used in [3]. Moreover, a hybrid BEM-FEM model, similar to that adopted in [4], is used to make the description of the flow inside the thinnest part of the jet simpler and robust.

2. TIME DOMAIN NUMERICAL SOLVER

The free surface flow generated by the water entry of a two-dimensional flat plate is simulated numerically through a mixed Eulerian-Lagrangian approach. Let φ denote the velocity potential, y the vertical coordinate with the y-axis pointing upwards and the x-axis coinciding with the undisturbed free surface oriented toward the right. By assuming gravity and surface tension effects negligible, the governing equations are

$$\begin{array}{rcll} \Delta\varphi &=& 0 & \Omega \\ \varphi_n &=& -V n_y & S_B \\ \dfrac{D\varphi}{Dt} &=& \dfrac{|\nabla\varphi|^2}{2} & S_S \\ \dfrac{D\boldsymbol{x}}{Dt} &=& \boldsymbol{u} & S_S\ , \end{array} \tag{1}$$

where V is the entry velocity of the plate, which is assumed to be constant, Ω is the fluid domain, S_S the free surface, S_B the plate contour, $\boldsymbol{n}$ the inward normal unit vector, $\boldsymbol{u}$ the fluid velocity (Fig. 1). In the numerical solution the symmetry condition along the plane $x = 0$ is exploited.

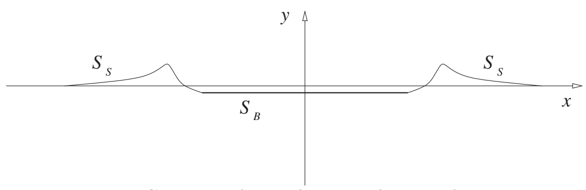

Figure 1: Sketch of the free surface deformation induced by the plate impact.

In addition to the above set of equations, further constraints are enforced at the plate ends, requiring that the free surface be attached to the edge and leave the plate tangentially. For the right hand side of the plate such constraints are expressed by the equations

$$\lim_{x \to L^+} \eta(x,t) = -Vt \quad , \quad \lim_{x \to L^+} \frac{\partial \eta(x,t)}{\partial x} = 0 \tag{2}$$

where $\eta(x,t)$ is the free surface elevation and $2L$ is the plate width.

At each step the velocity potential is written in terms of an integral representation

$$\varphi(P) = -\int_{S_B \cup S_S} (\varphi G_n - \varphi_n G) \; dS \;\; , \qquad P \in \Omega \tag{3}$$

where $G(P,Q) = \frac{1}{2\pi}\log(|P-Q|)$ is the free space Green function for the 2D Laplace operator. By taking the limit of equation (3) as P approaches the boundary of the fluid domain, an integral equation for the velocity potential and its normal derivative is obtained, solution of which provides the velocity potential along the plate and the normal derivative of the velocity potential along the free surface.

The solution scheme is arranged in two steps: first, at a specified time instant t the boundary value problem is solved, thus providing the value of the velocity potential and of its normal derivative throughout the domain boundary. Through differentiation of the potential along the boundary, the tangential velocity component is evaluated and then the velocity field on the free surface is completely determined. Next, the second step of the solution scheme is performed: the dynamic and kinematic free surface conditions are integrated in time for a set of Lagrangian markers lying on the free surface, thus obtaining the new free surface configuration and the distribution of the velocity potential along it, allowing to solve the boundary value problem for the new configuration.

The system of governing equation is integrated in time through a second order Runge-Kutta scheme. In order to enforce the additional conditions (2), at the first step of the Runge-Kutta scheme the normal velocity at the first panel attached to the plate is set to be equal to that along the plate. From the solution of the boundary value problem the velocity potential on the panel is derived which is used as a starting value for the second step of the Runge-Kutta scheme. At the end of each time step the panel distribution along the free surface is reinitialized. To this aim a cubic spline is built along the panel centroids and the panel distribution is reinitialized starting from the plate edge. Several constraints are enforced to the local panel size in order to achieve the best compromise among accuracy and computational effort.

From the computational standpoint the problem is very complicated due to the presence of the thin jet developing at the plate edges. An accurate description of the flow in this thin region would require a panel size of the order of the jet thickness which would imply a huge computational effort for the description of such small part of the fluid domain. A significant reduction of the computational effort can be achieved through a hybrid BEM-FEM approach [4]. At each step the region where the angle between the left and right boundaries of the jet is less than a treshold angle, say four degrees, is identified. Inside this region, a set of control volumes are defined on the basis of the panel discretization and within each one a bilinear representation of the velocity potential is constructed. From this representation the velocity components are derived and used to move the panel centroids.

To start the numerical solution, a proper scaling of the self-similar solution derived in [3] for small times has been used. To this aim, an initial time is fixed to a small value, say t^* (which corresponds to an initial plate depth h^*) and the variable scaling defined in [3] is used to scale the free surface shape and the associated velocity potential from the self-similar variables to the physical variables x, y, φ. As the solution derived in [3] is valid under the small time limit, higher order terms were neglected. As a consequence, small adjustments are needed in order to enforce the zero free surface elevation at the far field boundary. In the numerical calculations the far field boundary is located at $x = 1000$.

In order to evaluate the unsteady contribution to the pressure field along the plate the time derivative of the velocity potential $\dot{\varphi}$ is written in the form of an integral representation similar to (3). A boundary value problem is then derived by taking the limit of the integral representation as P approaches the boundary of the fluid domain. The time derivative of the velocity potential is assigned along the free surface whereas $\dot{\varphi}_n$ assigned on the plate [5].

3. SMALL TIME ASYMPTOTICS OF THE HYDRODYNAMIC LOADS

The initial asymptotics of the hydrodynamic loads acting on a flat plate impacting the water surface was derived in [1]. Therein, the second-order velocity potential along the plate was presented in the form

$$\varphi = -\dot{h}\sqrt{1-x^2} + \frac{h\dot{h}/2}{1-x^2} - \frac{h^{\frac{2}{3}}\dot{h}\tilde{C}_0}{\sqrt{1-x^2}} - h\dot{h} + o(t), \tag{4}$$

where $\tilde{C}_0 = 2|C_1|(3/\sqrt{2})^{\frac{2}{3}}$. The constant $C_1 = -0.41795$ is the coefficient of the eigensolution that characterizes the first-order inner solution. This constant was derived numerically in [3]. The pressure field associated to the outer velocity potential (4) is given by

$$\begin{aligned} p(x,0,t) &= \ddot{h}\sqrt{1-x^2} + \dot{h}^2 - \frac{\dot{h}^2}{1-x^2} + \\ &+ \frac{2}{3}\tilde{C}_0\dot{h}^2 h^{-\frac{1}{3}}\frac{1}{\sqrt{1-x^2}} + o(1). \end{aligned} \tag{5}$$

which is singular and not integrable at the plate edge.

This problem was overtaken by deriving the pressure field associated to the inner solution of the first-order problem. Under the change of variables

$$x = 1 + a(t)u \;\; , \; y = a(t)v \;\; , \; \varphi(x,y,t) = \sqrt{2}a^{1/2}\dot{h}\phi(u,v)$$

where $a(t) = [3/\sqrt{2}\dot{h}]^{2/3}$, the inner pressure field was presented as

$$p(u,0,t) = -\frac{\dot{h}^2}{a}\Big[\frac{2C_1}{\sqrt{-u}+\beta} + S(u) + o(1)\Big], \tag{6}$$

with $\beta = (4|C_1|)^{-1}$ and

$$S(u) = \phi_u^2 + \phi - 2u\phi_u - \frac{2C_1}{\sqrt{-u}+\beta} \, . \tag{7}$$

The function $S(u)$ has been evaluated from the inner solution derived in [3] and its graph is drawn in Fig. 2. Due to the equation $p(0,0,t) = 0$, the theoretical value of $S(0)$ is equal to $8C_1^2 \approx 1.39745762$. The numerical estimate, based on the solution given in [3] provides $S(0) \approx 1.145$.

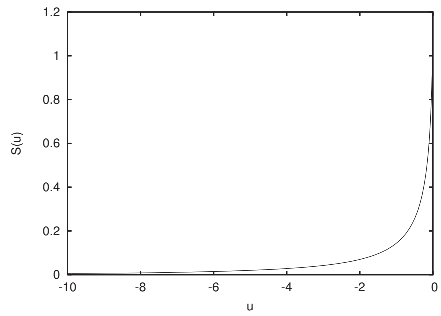

Figure 2: Graph of the function $S(u)$

Starting from the above considerations, the hydrodynamic force is evaluated by dividing the plate surface into two regions: the main region, where $0 < x < 1 - a\lambda$, and the inner one, where $1 - a\lambda < x < 1$. Here λ is a large parameter such that $\lambda \gg 1$ but $a\lambda^{\frac{3}{2}} \ll 1$. Then the total force acting on the plate is calculated as

$$F(t) = \lim[F_{main}(t) + F_{inner}(t)] + o(1), \qquad (8)$$

with the limit taken as $a \to 0$, $\lambda \to \infty$ and $a\lambda^{3/2} \to 0$. It can be shown that the contribution of the inner pressure is

$$F_{inner}(t) = 4|C_1|\dot{h}^2 \int_{-\lambda}^{0} \frac{\mathrm{d}u}{\sqrt{-u} + \beta} - 2\dot{h}^2 J + o(1), \qquad (9)$$

where

$$J = \int_{-\infty}^{0} S(u)\mathrm{d}u$$

and

$$\int_{-\lambda}^{0} \frac{\mathrm{d}u}{\sqrt{-u} + \beta} = 2\sqrt{\lambda} - \beta \ln \lambda + 2\beta \ln \beta + o(1)\ , \qquad (10)$$

whereas the contribution of the second-order outer pressure field is:

$$F_{main}(t) = \frac{\pi}{2}\ddot{h} + \dot{h}^2\Big[2 - \ln 2 + \frac{2}{3}\ln B\Big]$$

$$+\frac{2}{3}\dot{h}^2 \ln h + \dot{h}^2 \ln \lambda + \frac{2\pi}{3}\tilde{C}_0 \dot{h}^2 h^{-\frac{1}{3}} - 8|C_1|\dot{h}^2\sqrt{\lambda} + o(1)\ . \qquad (11)$$

From equations (9, 11) we finally obtain

$$F(t) = \frac{\pi}{2}\ddot{h} + \gamma \dot{h}^2 h^{-\frac{1}{3}} + \frac{2}{3}\dot{h}^2 \ln h$$

$$+\dot{h}^2\Big[2 - 2\ln(4|C_1|) - \ln 2 + \frac{2}{3}\ln B - 2J\Big] + o(1), \qquad (12)$$

where $\gamma = \frac{4\pi}{3}|C_1|B^{\frac{2}{3}}$. The integral of the function $S(u)$ provides $J \simeq 0.70629$.

In (12) all variables are non-dimensional. In dimensional variables (see [1]) this formula takes the form

$$F(t) = m_a \ddot{h} + \rho_0 \dot{h}^2 f(h/L),$$

where the penetration depth h, the time t and the force F are dimensional now, $m_a = \pi\rho_0 L^2/2$ is the added mass of the plate, ρ_0 is the liquid density,

$$f(x) = a_1 x^{-\frac{1}{3}} + \frac{2}{3}\ln x + a_0,$$

$$a_1 = 2.89035, \qquad a_0 = -0.63217.$$

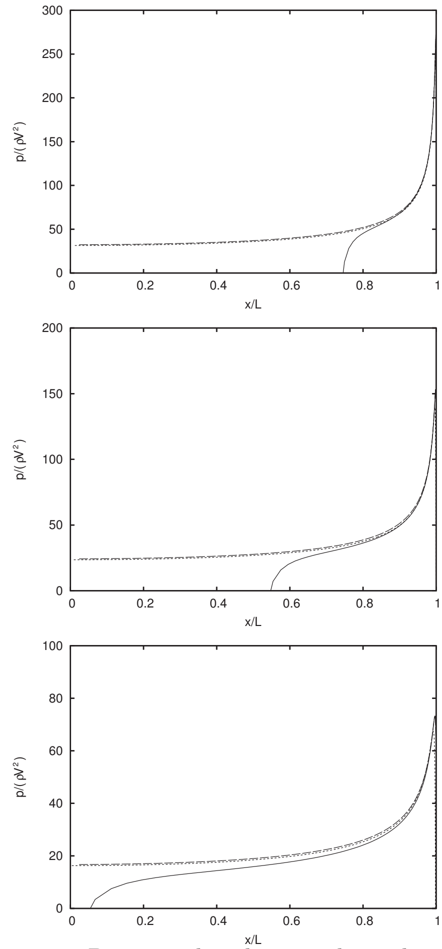

Figure 3: Pressure distribution along the plate at three different time instants: $t = 2.51e-5, 5.96e-5, 18.02e-5$. The solid line is the inner pressure field given by eq. (6), the dot line is the outer pressure field given by eq. (5) and the dash line is the numerical result.

4. NUMERICAL RESULTS

Calculations are performed for constant velocity of the plate and in non-dimensional variables.

In Fig. 3 the pressure field along the plate is shown at three different time instants, i.e. plate depths. In establishing the comparison the initial time shift of the numerical solution t^* has been accounted for: if t^N is the time elapsed in the numerical solution, the comparison has to be established with the theoretical solution at time $t = t^* + t^N$. In this paper we used $t^* = 1.5e-5$. For the same curves, a close up view about the plate edge is drawn in Fig. 4. From the figures it can be clearly seen that the inner pressure has a relevant role about the plate edge as it removes the singularity of the outer pressure field. Far from the plate edge, the inner solution fails. However, this happen there where the outer pressure field is already valid.

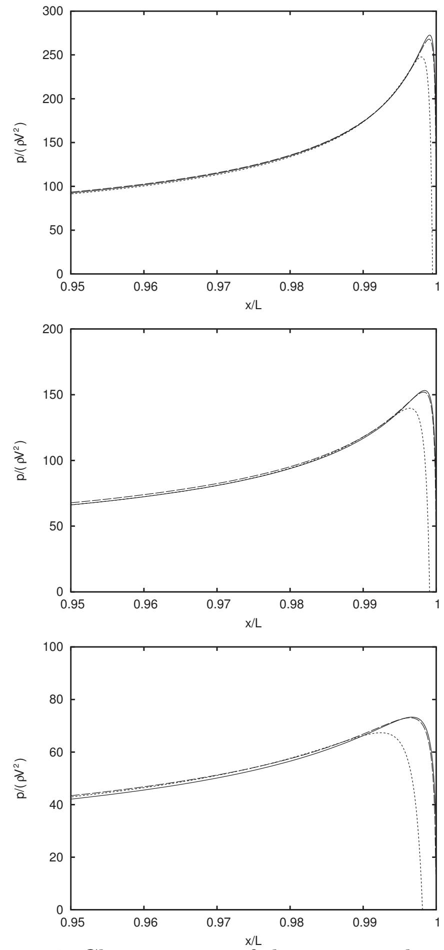

Figure 4: Close up view of the pressure distribution about the plate tip.

In Fig. 5 the total vertical force acting on the plate are drawn. The figure shows a very good agreement between the numerical and theoretical estimate, during the early stage of the penetration. Afterwards, the approximations made in deriving the small time solution fail. In Fig. 6 the relative difference between the theoretical and numerical estimates is shown. The figure indicates that the difference between the numerical and theoretical values of the vertical load is few per cent up to $t \approx 1/100$. The good agreement between the theoretical and numerical estimate makes it possible to use the theoretical estimate for the evaluation of the hydrodynamic loads in the very early stage of the impact process when numerical results are not available.

7. ACKNOWLEDGEMENTS

The work has been done in the framework of the *Programma Ricerche INSEAN Lug 2006-Dic 2007* financially supported by the Italian *Ministero dei Trasporti*. AAK acknowledges support from projects 2.12SBRAS and NSH-5873.2006.1.

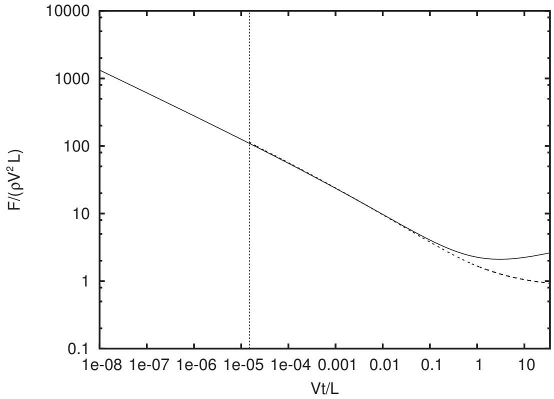

Figure 5: Time history of the nondimensional vertical force acting on the plate. The numerical result (dash line) are only available for $t > t^*$ (vertical line). The log scale of the axes has been used.

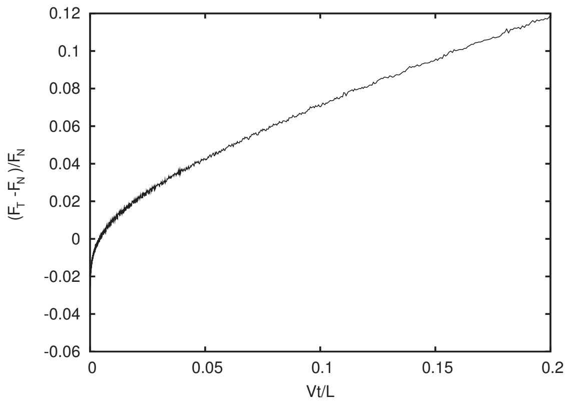

Figure 6: Time history of the relative difference between the theoretical and the numerical estimates.

8. REFERENCES

[1] A.A. Korobkin and A. Iafrati (2006) *Hydrodynamic loads on flat plate entering water*, *21st* IWWWFB, Loughborough, UK.

[2] A.A. Korobkin and A. Iafrati (2005) *Hydrodynamic loads during initial stage of floating body impact*, J. Fluids Struct., **21**, 413-427.

[3] A. Iafrati, A.A. Korobkin (2004) *Initial stage of flat plate impact onto liquid free surface*, Phys. Fluids, **16**, 2214-2227.

[4] D. Battistin and A. Iafrati (2004) *A numerical model for the jet flow generated by water impact*, J. Engng Math., **48**, 353-374.

[5] D. Battistin and A. Iafrati (2003) *Hydrodynamic loads during water entry of two-dimensional and axisymmetric bodies*, J. Fluids Struct., **17**, 643-664.